Brain Struct Funct (2017) 222:3007–3023
DOI 10.1007/s00429-017-1381-7

ORIGINAL ARTICLE

Co-localization of the cannabinoid type 1 receptor with corticotropin-releasing factor-containing afferents in the noradrenergic nucleus locus coeruleus: implications for the cognitive limb of the stress response

Ryan R. Wyrofsky[1] · Beverly A. S. Reyes[1] · Elisabeth J. Van Bockstaele[1]

Received: 22 March 2016 / Accepted: 31 January 2017 / Published online: 2 March 2017

Abstract The noradrenergic system has been shown to play a key role in the regulation of stress responses, arousal, mood, and emotional states. Corticotropin-releasing factor (CRF) is a primary mediator of stress-induced activation of noradrenergic neurons in the nucleus locus coeruleus (LC). The endocannabinoid (eCB) system also plays a key role in modulating stress responses, acting as an "anti-stress" neuro-mediator. In the present study, we investigated the cellular sites for interactions between the cannabinoid receptor type 1 (CB1r) and CRF in the LC. Immunofluorescence and high-resolution immunoelectron microscopy showed co-localization of CB1r and CRF in both the core and peri-LC areas. Semi-quantitative analysis revealed that 44% (208/468) of CRF-containing axon terminals in the core and 35% (104/294) in the peri-LC expressed CB1r, while 18% (85/468) of CRF-containing axon terminals in the core and 6.5% (19/294) in the peri-LC were presynaptic to CB1r-containing dendrites. In the LC core, CB1r + CRF axon terminals were more frequently of the symmetric (inhibitory) type; while in the peri-LC, a majority were of the asymmetric (excitatory) type. Triple label immunofluorescence results supported the ultrastructural analysis indicating that CB1r + CRF axon terminals contained either gamma amino butyric acid or glutamate. Finally, anterograde transport from the central nucleus of the amygdala revealed that CRF-amygdalar afferents projecting to the LC contain CB1r. Taken together, these results indicate that the eCB system is poised to directly modulate stress-integrative heterogeneous CRF afferents in the LC, some of which arise from limbic sources.

Keywords Norepinephrine · Psychiatric disorders · Arousal · Addiction

Introduction

The stress response is characterized by a coordinated set of endocrine, physiological, and cognitive responses to perceived threats in the environment (Ulrich-Lai and Herman 2009). A critical aspect of the endocrine stress response is the tight feedback regulation that serves to restrain and terminate the response (Keller-Wood and Dallman 1984), which when dysregulated, and contributes to the etiology of many stress-induced neuropsychiatric disorders (Plotsky et al. 1998; Wingenfeld and Wolf 2011). Feedback inhibition of the hypothalamic–pituitary–adrenal (HPA) axis by glucocorticoids is critical in terminating the endocrine limb of the stress response (Abou-Samra et al. 1986; Keller-Wood and Dallman 1984). However, other neural circuits involved in the stress response are differentially regulated (Herman and Cullinan 1997; Ulrich-Lai and Herman 2009).

Stressors that initiate the HPA response to stress also activate the brainstem locus coeruleus (LC)–norepinephrine (NE) system via the pro-stress neuropeptide, corticotropin-releasing factor (CRF) (Vale et al. 1981; Valentino 1988). CRF-immunoreactive axon terminals synapse onto LC–NE dendrites and arise from multiple limbic-related and autonomic-related brain areas (Aston-Jones et al. 1991; Van Bockstaele et al. 1996a, b, 1999). Stress-induced increases in CRF from these afferent sources can lead to inappropriate increases in the firing of LC–NE neurons and

✉ Ryan R. Wyrofsky
rrw47@drexel.edu

[1] Department of Pharmacology and Physiology, College of Medicine, Drexel University, 245 S. 15th Street, Philadelphia, PA 19102, USA

subsequent dysregulation of NE release in limbic and cortical areas (Curtis et al. 1996; Valentino et al. 2006; Van Bockstaele et al. 2010). The parallel engagement of the HPA and LC–NE systems serves to coordinate both endocrine and cognitive limbs of the stress response (Valentino and Van Bockstaele 2008a). One mechanism for counteracting stress responses in these neural circuits is through stress-elicited engagement of neuromodulators that act in opposition to pro-stress systems, such as engagement of the endogenous opioid system (Heilig 2004; Reyes et al. 2008a, 2011; Tjoumakaris et al. 2003; Torner et al. 2001; Valentino and Van Bockstaele 2001; Van Bockstaele et al. 2000). Identifying mechanisms and underlying counter-regulation of the stress response may better inform therapeutic strategies to prevent or treat stress-related neuropsychiatric diseases.

The endocannabinoid (eCB) system is considered as an "anti-stress" neuromodulator that modulates pro-stress responses through effects on synaptic activity (Cota 2008; Viveros et al. 2007). Extracts of *cannabis* have been used as stress-reducing medicinals throughout history and by many cultures to reduce anxiety, pain, seizures, mania, and muscle spasms (Zuardi 2006). Modern research confirms certain benefits, with constituents of *cannabis*, Δ^9-tetrahydrocannabinol (THC), and cannabidiol, being reported as effective anti-anxiety agents and stress-reducers (Bergamaschi et al. 2011; Tournier et al. 2003). Emerging evidence also supports a role for the eCB system in the modulation of stress responses through effects on synaptic activity. The eCB ligands, *N*-arachidonoylethanolamine/anandamide (AEA) and 2-arachidonoylglycerol (2-AG), are primarily synthesized postsynaptically in response to increases in intracellular Ca^{2+} or activation of phospholipase C β (Castillo et al. 2012; Di Marzo et al. 2004). Degradation of AEA and 2-AG occurs through the catabolic action of fatty acid amide hydrolase (FAAH) and monoacylglycerol lipase, respectively (Castillo et al. 2012; Di Marzo et al. 2004). Acting as retrograde messengers, AEA and 2-AG cross the synapse, where they primarily act through G_i-coupled cannabinoid CB1r localized to axon terminals (Castillo et al. 2012; Herkenham et al. 1990; Van Sickle et al. 2005), thereby inhibiting neurotransmitter release. By modulating glutamatergic and gamma amino butyric acid (GABA) ergic release, CB1r exert a profound effect on postsynaptic neuronal activity (Freund et al. 2003).

CB1r protein and mRNA have been localized to the LC (Derbenev et al. 2004; Herkenham et al. 1991; Mailleux and Vanderhaeghen 1992; Matsuda et al. 1993). At the ultrastructural level, CB1rs in the LC have been shown to be localized both presynaptically in axon terminals targeting NE-containing neurons as well as postsynaptically in somatodendritic processes (Scavone et al. 2010). Electron microscopy studies have shown that presynaptically distributed CB1r are localized to both excitatory- and inhibitory-type synapses (Scavone et al. 2010), which is consistent with electrophysiological studies. Systemic administration of CB1r agonists (Muntoni et al. 2006) and fatty acid amide hydrolase (FAAH) inhibitors (Gobbi et al. 2005) increase the firing rate of un-stimulated noradrenergic neurons in the LC in a CB1r-dependent manner. CB1r agonists also increase cFos expression in the LC (Oropeza et al. 2005; Patel and Hillard 2003), enhance *N*-methyl-D-aspartate (NMDA)-induced firing of LC neurons (Mendiguren and Pineda 2004), and increase NE synthesis (Moranta et al. 2009) and release (Oropeza et al. 2005) in terminal regions. WIN 55212-2 suppresses the inhibition of LC firing induced by activation of GABAergic afferents to the LC (Muntoni et al. 2006). Taken together, these results are consistent with a mechanism by which activation of CB1r on excitatory- or inhibitory-type terminals in the LC results in increases in the firing of noradrenergic neurons. However, local administration of CB1r agonists into the LC does not alter the spontaneous firing of LC neurons (Mendiguren and Pineda 2006) suggesting an indirect effect of CB1r agonists on LC firing, perhaps through increased afferent activity into the LC.

Convergent lines of evidence support a suppressive CB1r mechanism on CRF. CRF-induced activation of the sympathetic nervous system is inhibited by CB1r agonist administration and is potentiated by CB1r antagonists (Shimizu et al. 2010). Activation of glucocorticoid receptors by cortisol causes an increase in eCB production, which then activates CB1r on presynaptic glutamatergic neurons within the paraventricular nucleus of the hypothalamus (PVN) resulting in a decrease in hypothalamic release of CRF (Hill et al. 2010). In addition, a longer feedback loop exists, where activation of CB1r on GABA neurons within the prelimbic medial prefrontal cortex (mPFC) causes a disinhibition of GABAergic neurons in the bed nucleus of the stria terminalis (BNST) which then project to the PVN, ultimately leading to a decrease in CRF release (Hill and McEwen 2009; Hill et al. 2010). Because of the complex interaction of the eCB system on stress-related circuitry and the localization of both CB1r and CRF afferents within the LC, we sought to examine anatomical substrates for putative interactions between CB1r and CRF in the LC. Therefore, the present study used light microscopy, confocal fluorescence microscopy, and high-resolution immunoelectron microscopy to define how CB1r may be positioned to regulate CRF afferents in the LC.

Methods

Animals

For all experiments, male Sprague–Dawley rats between 200 and 300 g (Jackson Laboratory, Sacramento, CA) were used. They were housed two per cage, under the standard conditions (25 °C temperatures) and a 12 h light/dark cycle (lights turned on at 7:00 am). Ad libitum access to food and water was provided, and animal protocols were approved by the Drexel University College of Medicine Institutional Animal Care and Use Committee in accordance with the revised Guide for the Care and Use of Laboratory Animals (1996). All efforts were made to utilize only the minimum number of animals necessary to produce reliable scientific data.

Immunofluorescence

Rats were deeply anesthetized via isoflurane exposure (Vedco, Inc., St. Joseph, MO) in a holding cage. Once a sufficient level of anesthesia was achieved, rats were then transcardially perfused via the ascending aorta with heparin followed by a 4% formaldehyde solution in 0.1 M phosphate buffer (PB; pH 7.4). Brains were then dissected, post-fixed in the formaldehyde solution for 24 h, and placed in 30% sucrose and 0.1 M PB solution before sectioning. Forty micrometer sections through the rostrocaudal extent of each brain were collected using a cryostat (Microm HM 50, Microm International GmbH, Walldorf, Germany). Serial sections through the LC were placed in 1% sodium borohydride in 0.1 M PB for 30 min to remove any aldehydes remaining from the perfusion, followed by a 30 min incubation in 0.5% bovine serum albumin (BSA) in 0.1 M Tris buffered saline (TBS; pH 7.6). Following extensive rinsing in 0.1 M TBS, tissues were incubated overnight in a mixture of primary antibodies including (Table 1): CRF peptide raised in guinea-pig (1:7000, Peninsula Laboratories, San Carlos, CA), CB1r raised in rabbit (1:1000, kindly provided by Dr. Ken Mackie, Indiana University, IN), vesicular glutamate transporter (VGlut) raised in mouse (1:4000, Synaptic Systems, Gottingen, Germany), glutamate decarboxylase (GAD) raised in goat (1:700, Santa Cruz, Santa Cruz, CA), synaptophysin (Syn) raised in mouse (1:500, Merck Millipore, Billerica, MA), tyrosine hydroxylase (TH) raised in mouse (1:5000, Immunostar, Hudson, WI), and unconjugated Phaseolus Vulgaris Leucoagglutinin (PHAL) raised in goat (1:5000, Vector Laboratories, Burlingame, CA). For the primary antibodies that have not been previously characterized by our laboratory (VGlut, GAD, PHAL, and Syn), serial dilutions were performed to determine the optimal antibody concentration for the experiments. To visualize proteins, the following secondary antibodies were used, all at a concentration of 1:400 (Jackson ImmunoResearch): rhodamine isothiocyanate (TRITC) conjugated donkey anti-rabbit, fluorescein isothiocyanate (FITC) conjugated donkey anti-mouse, FITC conjugated donkey anti-goat, Alexafluor 647 conjugated donkey anti-guinea-pig, and Alexafluor 647 conjugated donkey anti-mouse. In addition, some tissue sections were also incubated with 4′,6-diamidino-2-phenylindole (DAPI; EMD Millipore, Billerica, MA) at 1:10,000 for 5 min and washed three times with 0.05 M PB. The tissue sections were then examined using a Olympus IX81 inverted microscope (Olympus, Hatagaya, Shibuya-Ku, Tokyo, Japan) equipped with lasers (Helium Neon laser and Argon laser; models GLG 7000; GLS 5414A and GLG 3135, Showa Optronics Co., Tokyo, Japan) with the excitation wavelength of 488, 543, and 635. The microscope is also equipped with filters (DM 405-44; BA 505-605; and BA 560-660) and

Table 1 Characterization of the primary antibodies used for immunofluorescence microscopy (IF) and electron microscopy (EM)

Antigen	Immunogen	Host	Source	Catalog #	Dilution	References
TH	TH purified from rat PC12 cells	Mouse	Immunostar Inc	22941	1:5000 (IF)	Van Bockstaele and Pickel (1993), Oropeza et al. (2005)
CBIr	Last 15 aa of the C terminal of the rat CB1r	Rabbit	Dr. Ken Mackie	n/a	1:1000 (IF and EM)	Carvalho et al. (2010), Scavone et al. (2010)
CRF	Synthetic CRF peptide	Guinea-pig	Peninsula Laboratories	T-5007	1:7000 (IF) 1:2000 (EM)	Rudoy et al. (2009)
VGlutl	aa 456–560 of Strep-Tag fusion protein of rat VGlutl	Mouse	Synaptic systems	135 311	1:4000 (IF)	Javadi et al. (2015)
GAD-65/67	C terminus of human GAD-67	Goat	Santa Cruz	sc-7513	1:700 (IF)	Papay et al. (2006), Rubio-Aliaga et al. (2004)
Syn	Rat retina synaptophysin	Mouse	Millipore	MAB368	1:500 (IF)	Yamanaka et al. (2011)
PHAL	Red kidney bean lectin receptor specific	Goat	Vector laboratories	AS-2224	1:5000 (IF)	Van Bockstaele et al. (2001)

with Olympus Fluoview ASW FV1000 program (Olympus, Hatagaya, Shibuya-Ku, Tokyo, Japan). Analysis of co-localization of profiles was obtained from dually labeled immunofluorescence images of CB1r and CRF taken from alternate LC sections of three rats ($n=3$) via the Coloc2 plug-in on the FIJI ImageJ software. CRF (green) was set to channel 1, and CB1r (red) was set to channel 2, so the Pearson's coefficients obtained are representative of the likelihood that CB1r is co-localized with respect to CRF. To best visualize co-localization in fluorescence micrographs, CB1r was always pseudocolored red, CRF and Syn, pseudocolored green, and glutamic acid decarboxylase (GAD) and vesicular glutamate transporter (VGlut) were pseudocolored cyan. Two sets of control tissues were processed in parallel, one with the omission of primary antibodies and the other with the omission of secondary antibodies. As an additional control, rabbit anti-CB1r was processed with both TRITC conjugated donkey anti-rabbit and Alexafluor 647 conjugated donkey anti-guinea-pig, and guinea-pig anti-CRF was also processed with both TRITC conjugated donkey anti-rabbit and Alexafluor 647 conjugated donkey anti-guinea-pig (Fig. 1). Since secondary antibody fluorescence was only observed when the corresponding primary antibody was used, there is no detectable cross reactivity between the antibodies.

Anterograde transport

Surgery was performed on male Sprague–Dawley rats ($n=3$). Animals injected with PHAL into the central nucleus of the amygdala (CeA) were initially anesthetized with a cocktail of ketamine hydroxide (100 mg/kg; Phoenix Pharmaceutical, Inc., St. Joseph, MO) and xylazine (2 mg/kg; Phoenix Pharmaceutical, Inc., St. Joseph, MO) in saline intraperitoneally (i.p.) and placed in a stereotaxic apparatus for surgery. Anesthesia was supplemented with isoflurane (Abbott Laboratories, North Chicago, IL; 0.5–1.0%, in the air) via a specialized nose cone affixed to the incisor

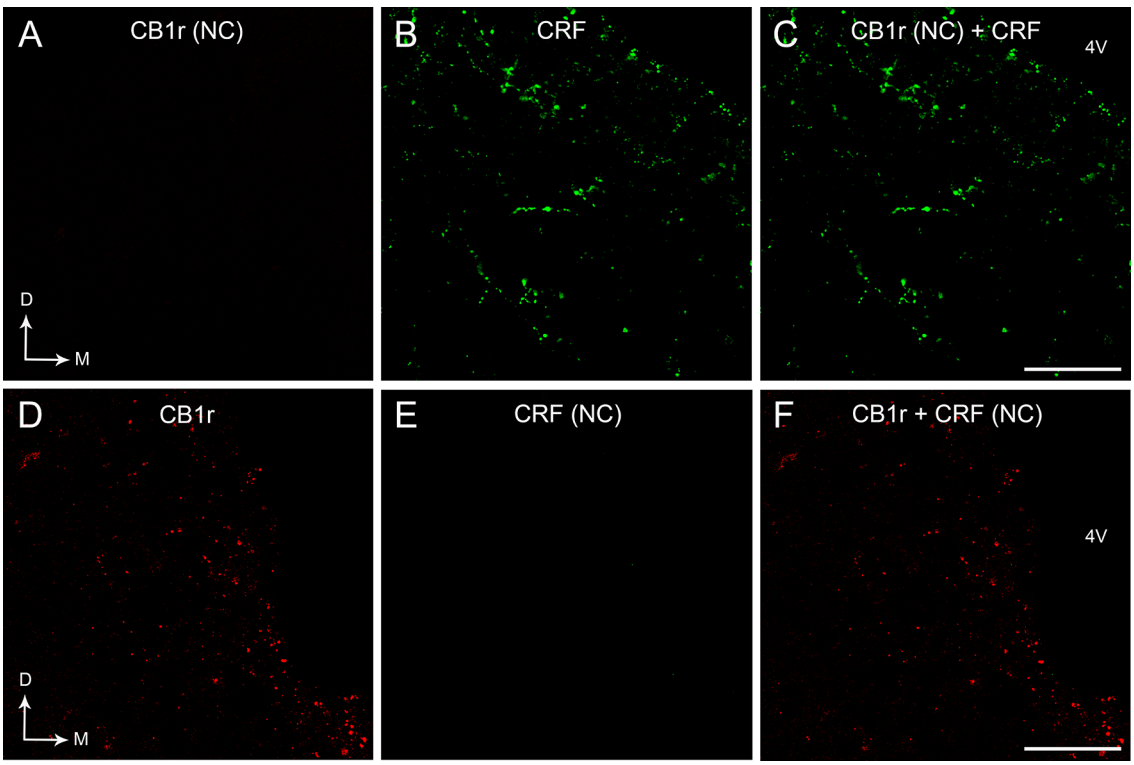

Fig. 1 Secondary antibodies show no cross reactivity. Confocal fluorescence micrographs of control experiments that were performed to examine rhodamine isothiocyanate (TRITC)- and Alexafluor 647-conjugated secondary antibody specificity. **a**–**c** Tissue was processed with guinea-pig anti-CRF primary antibody, then both Alexafluor 647-conjugated donkey anti-guinea-pig and TRITC-conjugated donkey anti-rabbit secondary antibodies. **d**–**f** Tissue was processed with rabbit anti-CB1r primary antibody, then both TRITC conjugated donkey anti-rabbit and Alexafluor 647 conjugated donkey anti-guinea-pig secondary antibodies. **a** With the absence of rabbit anti-CB1r primary antibody, TRITC does not fluoresce. **b** CRF (*green*) peptide is visualized by Alexafluor 647 fluorescence. **c** Merging of TRITC and Alexafluor 647 channels. **d** CB1r (*red*) is visualized by TRITC fluorescence. **e** With the absence of guinea-pig anti-CRF primary antibody, Alexafluor 647 does not fluoresce. **f** Merging of TRITC and Alexafluor 647 channels. In **a** and **e**, minimal non-specific background labeling is observed. This demonstrates the specificity of both TRITC and Alexafluor secondary antibodies for their respective primary antibodies, and does not show any cross reactivity

bar of the stereotaxic frame (Stoelting Corp., Wood Dale, IL). Glass micropipettes (Kwik-Fil, 1.2 mm outer diameter; World Precision Instruments, Inc., Sarasota, FL) with tip diameters of 15–20 µm were filled with 2.5% PHAL (Vector Laboratories, Burlingame, CA). The tips of the glass micropipettes were positioned in the CeA using the following coordinates: 2.3 mm posterior from Bregma and 4.2 mm medial/lateral based on the rat brain atlas of Paxinos and Watson (1997). The glass micropipettes were lowered targeting the appropriate coordinates for placement of PHAL into the CeA (6.7 mm ventral from the top of the skull), and PHAL was injected using a Picospritzer (General Valve Corporation, Fairfield, NJ) at 24–26 psi, 10 ms duration and 0.2 Hz. Injection of PHAL was done unilaterally into the CeA of each animal. Pipettes were left at the site of injection for 5 min after tracer deposit to limit leakage of the tracer along the pipette track. After 10 days, rats were anesthetized and perfused as described above, and tissue was processed for immunohistochemical detection of PHAL, CB1r, and CRF.

Electron microscopy

Rats were anesthetized and perfused as described above, using a 2% formaldehyde and 3.75% acrolein (from Electron Microscopy Sciences) solution. Brains were post-fixed in the formaldehyde and acrolein solution for 24 h, and 40 µm sections were cut on a vibratome (Pelco EasiSlicer, Ted Pella, Inc., Redding, CA). Tissues were processed as we previously described (Reyes et al. 2006a, b; Scavone et al. 2011). Briefly, alternate sections through the LC were processed for CRF and CB1r ($n=4$). Tissues were placed in 1% sodium borohydride in 0.1 M PB (pH 7.4) for 30 min to remove any aldehydes remaining from the perfusion, followed by a 30-min incubation in 0.5% BSA in 0.01 M TBS. They were then rinsed with TBS and incubated overnight with CRF peptide antibody raised in guinea-pig (1:2000, Peninsula Laboratories) and CB1r antibody raised in rabbit (1:1000). CRF was then visualized with immunoperoxidase labeling via biotinylated donkey anti-guinea-pig antibodies (1:400) for 30 min, followed by an avidin–biotin incubation for 30 min (ABC kit, Vector Laboratories, Burlingame, CA), and visualization with a 5-min reaction in 3,3′-diaminobenzidine (DAB; Sigma–Aldrich Inc., St. Louis, MO) and hydrogen peroxide in 0.1 TBS.

CB1r was visualized through immunogold–silver enhancement. Tissues were first washed extensively, then incubated in goat anti-rabbit IgG, conjugated to 1 nm gold particles (Amersham Bioscience Corp., Piscataway, NJ) for 2 h. Next, tissues were washed in 0.2% gelatin-phosphate buffered saline (PBS) and 0.8% BSA buffer followed by 0.1 M PBS, then incubated for 10 min in 2% glutaraldehyde (Electron Microscopy Sciences, Hatfield, PA) in 0.01 M PBS. After washing with 0.01 M PBS and 0.2 M sodium citrate buffer (pH 7.4) sequentially, silver enhancement of the gold particles was done using a silver enhancement kit (Amersham Bioscience Corp.). This process was optimized empirically to determine the optimal enhancement time, which ranged between 5 and 8 min. Tissues were then washed again in 0.2 M citrate buffer and 0.1 M PB, then incubated in 2% osmium tetroxide (Electron Microscopy Sciences) in 0.1 M PB. After a 1 h incubation, tissues were washed in 0.1 M PB, dehydrated in ascending series of ethanol then propylene oxide, and flat embedded in Epon 812 between two sheets of aclar (Electron Microscopy Sciences). Sections were cut at 70 nm on a Leica Ultracut (Leica Microsystems, Wien, Vienna, Austria) with a diamond knife (Diatome-US, Fort Washington, PA), collected on copper mesh grids, and examined with an electron microscope (Morgagni Fei Company, Hillsboro, OR), with digital images captured by an AMT advantage HR/HR-B CCD camera system (Advance Microscopy Techniques Corp, Danvers, MA). Tissue was processed with the reverse immunolabels for each primary antibody, with CRF immunolabeled with silver-intensified gold particles and CB1r with peroxidase.

Controls and data analysis

Tissue sections for electron microscopy were obtained from rats with the best immunohistochemical labeling and preservation of ultrastructural morphology. The semi-quantitative approach used in the present study is well established and has been described previously (Reyes et al. 2006b, 2007; Van Bockstaele et al. 1996a, b). While acrolein fixation optimizes the preservation of ultrastructural morphology, the caveat of limited and or differential penetration of immunoreagents in thick tissue sections exists (Chan et al. 1990; Leranth and Pickel 1989). Consequently, the limited penetration of CB1r and CRF may result in an underestimation of the relative frequencies of their distribution. We mitigated this limitation by collecting the tissue sections exclusively near the tissue–Epon interface, where penetration is maximal and profile was sampled only when all the markers were present in the surrounding neuropil included in the analysis. The cellular elements were identified based on the description of Peters and Palay (1996). Somata contained a nucleus, Golgi apparatus, and smooth endoplasmic reticulum. Proximal dendrites contained endoplasmic reticulum, were postsynaptic to axon terminals and were larger than 0.7 µm in diameter. A terminal was considered to form a synapse if it showed a junctional complex, a restricted zone of parallel membranes with slight enlargement of the intercellular space, and/or associated with postsynaptic thickening. A synaptic specialization was only limited to the profiles that form clear morphological characteristics of

either Type I or Type II (Gray 1959). Asymmetric synapses were identified by thick postsynaptic densities (Gray's type I; Gray 1959). In contrast, symmetric synapses had thin densities (Gray's type II; Gray 1959) both pre- and postsynaptically. An undefined synapse was defined as an axon terminal plasma membrane juxtaposed to that of a dendrite or soma devoid of recognizable membrane specializations and no intervening glial processes. Two individuals quantified the synapse distributions in all profiles analyzed, both reaching the same percentages.

Identification of immunogold–silver labeling in profiles

Selective immunogold–silver labeled profiles were identified by the presence, in single thin sections, of at least two immunogold–silver particles within a cellular compartment. As we previously reported (Reyes et al. 2006b, 2007; Van Bockstaele et al. 1996a, b), single spurious immunogold–silver labeling can contribute to false positive labeling and can be detected on blood vessels, myelin, or nuclei. Although minimal spurious labeling was identified in the present study, the criterion for considering an axon or dendrite immunogold–silver labeled was defined by the presence of at least two silver particles in a profile. Whenever possible, the more lightly labeled dendritic labeling for CRF was confirmed by detection in at least two adjacent sections. Profiles containing CRF-labeled axon terminals were counted and their association with CB1r receptors was determined.

Results

CB1r localization in LC: coexistence with CRF

The LC is a compact cluster of NE neurons in the dorsal pons that serves as the primary source of NE in forebrain regions such as the hippocampus and cortex that govern cognition, memory, and complex behaviors. To examine the relationship of CB1r with presynaptic neural profiles, CB1r immunoreactivity was combined with immunolabeling of an axonal marker, synaptophysin (Syn). Syn is a SNARE protein that is localized to the plasma membrane of axonal terminals (Edelmann et al. 1995). Immunofluorescence microscopy was performed for CB1r and Syn in the LC and DAPI was used to denote the nuclei in the LC region (Fig. 2). Consistent with its known localization, Syn appeared in varicose processes, some of which were co-localized with CB1r (Fig. 2d) suggesting that CB1r is located presynaptically in axon terminals. There also existed areas of CB1r immunoreactivity lacking Syn immunoreactivity, suggesting that CB1r is associated with profiles other than axon terminals in the LC.

Considering the presynaptic distribution of CB1r, we sought to test the hypothesis that the eCB system is positioned to directly modulate CRF-containing afferents within the LC using immunofluorescence detection of CRF and CB1r (Fig. 3a–c). As previously described in independent studies (Scavone et al. 2010; Valentino et al. 1992; Van Bockstaele et al. 1996a, 1999), CB1r and CRF appeared in punctate varicose processes that were distributed in the

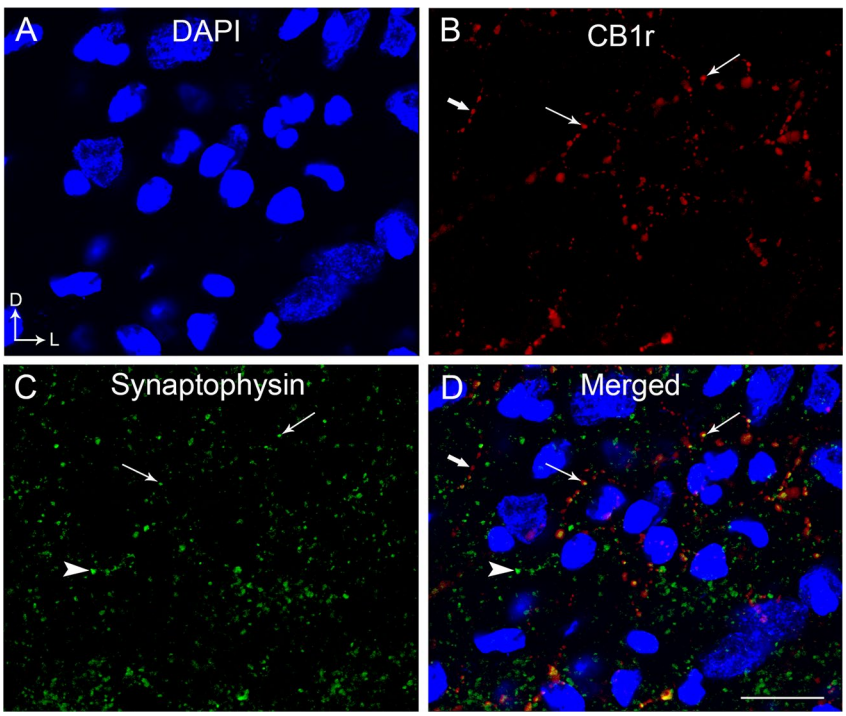

Fig. 2 CB1r is localized presynaptically in the LC. Confocal fluorescence micrographs showing that CB1r (*red*) and synaptophysin (Syn; *green*) are co-localized within the LC. **a** DAPI was used to detect nuclei in LC cell bodies, **b, c** CB1r was detected using a rhodamine isothiocyanate-conjugated secondary antibody, and Syn, an axonal marker, was detected using an Alexafluor 647-conjugated secondary antibody (pseudocolored in *green*). **d** CB1r and Syn appear punctate throughout. Co-localization of CB1r and Syn (*yellow*) can be seen in **d**. *Arrows* point to CB1r and Syn co-localization, while *arrowhead* and *thick arrow* point to singly labeled CB1r or Syn, respectively. *Arrows* indicate dorsal (*D*) and lateral (*L*) orientation. 4 V, fourth ventricle. *Scale bar* 25 µm

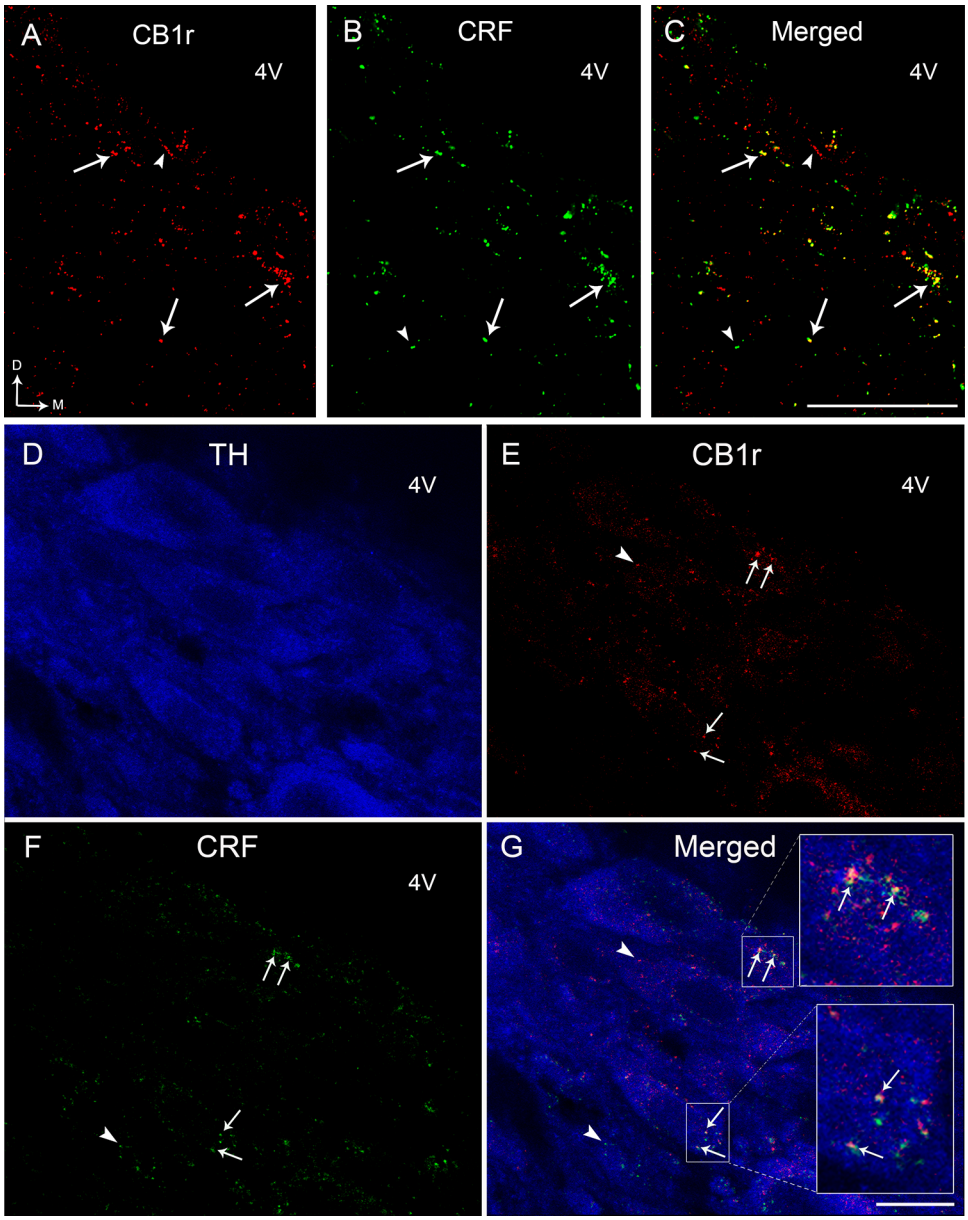

Fig. 3 CB1r is co-localized with CRF in the LC. Confocal fluorescence micrographs showing that CB1r (*red*) and CRF (*green*) are co-localized in the LC. CB1r was detected using a rhodamine isothiocyanate-conjugated secondary antibody (**a**) and CRF was detected using an Alexafluor 647-conjugated secondary antibody (pseudo-colored in *green*) (**b**). Co-localization of CB1r and CRF (*yellow*) is shown in a merged image in **c**. *Arrows* denote CB1r and CRF co-localization while *arrowheads* point to singly labeled CB1r and CRF. **d**–**g** TH, a marker for noradrenergic neurons, was detected using fluorescein isothiocyanate-conjugated secondary antibody (pseudo-colored in *blue*) and was used to show that co-existing CB1r and CRF axon terminals are present within the core of the LC. In addition, note that CB1r are localized to TH-containing neurons suggesting that CB1r are localized both pre- and post-synaptically in the LC. **g** *Insets* show co-localization of CB1r and CRF, and are shown at a higher magnification. *Arrows* depict triple co-localization of CB1r, CRF, and TH. 4 V, fourth ventricle. *Scale bar* 25 µm

LC. Triple immunofluorescence revealed co-localization of CB1r and CRF-immunoreactive processes adjacent to TH-immunoreactive neurons (Fig. 3d–g). These data also show the presence of CB1r in TH-containing neurons suggesting that CB1r is also found postsynaptically, confirming our previous studies demonstrating that CB1r is localized both pre- and postsynaptically, in the LC (Scavone et al. 2010).

The core of the LC consists of a dense cluster of noradrenergic neurons, with dendrites that extend into the surrounding area, known as the peri-LC (Shipley et al. 1996). CRF afferent nuclei are known to topographically innervate the LC (Van Bockstaele et al. 2001). CRF afferents from limbic regions, such as the amygdala and bed nucleus of the stria terminalis, have been shown to provide topographic innervation of the rostrolateral peri-LC, while medullary afferents have been shown to project primarily to the core (Valentino and Van Bockstaele 2008a; Van Bockstaele et al. 1996a, 1999). To determine if there is differential distribution between the eCB regulation of CRF afferents in the core vs. peri-LC, confocal images of CB1r and CRF immunoreactivity were analyzed using the imageJ plug-in coloc2, and the average Pearson's coefficient (PC) was determined: for the core, PC = 48.4 ± 3.12 and for the peri-LC, PC = 31.6 ± 3.78. PC values represent the linear correlation of CB1r (red) signal intensity with respect to CRF (green) signal intensity at each pixel, and a PC > 0 signifies that the signal co-localization is greater than it would be at random, with a PC = 1 indicating perfect correlation (Adler and Parmryd 2010). These values suggest that there is a correlation between CB1r and CRF in both the core and the

peri-LC. Analysis of co-localization was further carried out using immunoelectron microscopy.

Ultrastructural localization of CRF and CB1r in the LC

Immunoelectron microscopy was used to further determine the precise subcellular co-localization of CB1r in relation to CRF afferents in the LC (Fig. 4). Immunoperoxidase labeling was used for the detection of CRF, and immunogold–silver labeling was used for the detection of CB1r. These markers are routinely reversed, and results showed a similar distribution irrespective of the secondary immunolabel of the primary antibody. The core of the LC consists of a dense cluster of noradrenergic neurons, with dendrites that extend into the surrounding area, known as the peri-LC (Shipley et al. 1996). CRF afferent nuclei are known to topographically innervate the LC (Van Bockstaele et al. 2001). CRF afferents from limbic regions, such

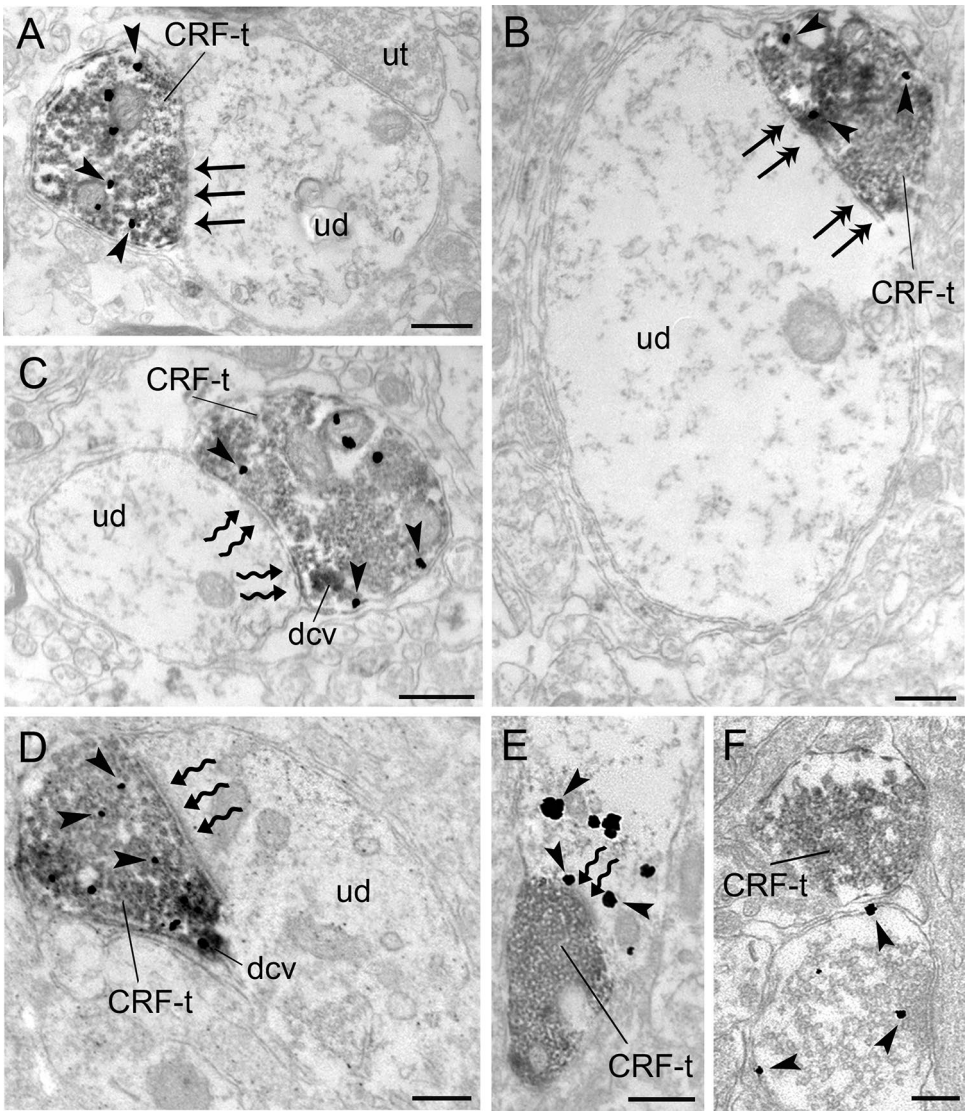

Fig. 4 CRF-containing afferents co-localize with CB1r in the LC. a–f. Representative electron micrographs showing immunoperoxidase labeling for CRF-containing axon terminals (CRF-t) and immunogold–silver labeling for CB1r (*arrowheads*) in the LC core (**a**–**c**) and peri-LC (**d, e**). **a** CRF-labeled axon terminal containing CB1r forms is in direct contact (*arrows*) with an unlabeled dendrite (ud) in the LC core. **b** Peroxidase-labeled CRF-t co-localizing CB1r (*arrowheads*) forms a symmetric-type synapse (*double arrows*) with an unlabeled dendrite (ud) in the LC core. **c** Axon terminal containing both peroxidase labeling for CRF and immunogold–silver labeling for CB1r (*arrowheads*) forms an asymmetric-type synapse (*zig zag arrows*) with an unlabeled dendrite (ud) in the LC core. **d** CRF-labeled axon terminal containing CB1r (*arrowheads*) forms an asymmetric-type synapse (*zig zag arrows*) with an unlabeled dendrite (ud) in the peri-LC. **e** Peroxidase-labeled CRF axon terminal forming an asymmetric synapse (*zig zag arrows*) with a dendrite containing immunogold–silver labeled CB1r (*arrowheads*) **f** Peroxidase-labeled CRF axon terminal can be seen in close proximity to a separate axon terminal containing immunogold–silver labeled CB1r. *dcv* dense core vesicle. *Scale bar* 0.5 µm

as the amygdala and bed nucleus of the stria terminalis, have been shown to provide topographic innervation of the rostrolateral peri-LC, while medullary afferents have been shown to project primarily to the core (Valentino and Van Bockstaele 2008a; Van Bockstaele et al. 1996a, 1999). To determine if there is differential distribution between the eCB regulation of CRF afferents in the core vs. peri-LC, electron micrographs from the core and the peri-LC were quantified separately.

For analysis of the LC core, a total of 468 profiles were analyzed from at least five grids per LC section. At least three LC sections were collected from each Sprague–Dawley rat ($n=4$). Several interactions between CB1r and CRF-containing axon terminals were observed. One type of interaction demonstrated axon terminals containing both CB1r and CRF, suggesting an anatomical substrate for presynaptic modulation of CRF by CB1r (Fig. 4a–d). It was also observed that CRF-containing afferents target dendrites expressing CB1r, providing a cellular substrate for potential postsynaptic effects (Fig. 4e). Of the 468 CRF-labeled axon terminals analyzed, 44.4% (208/468 profiles) also contained CB1r and of the 208 CRF + CB1r co-labeled axon terminals and 12.5% (26/208 profiles) contacted dendrites that expressed CB1r postsynaptically. In addition, 18.2% (85/468 profiles) of CRF axon terminals that did not express CB1r synapsed onto dendrites that contained CB1r. The remainder of CRF terminals did not exhibit CB1r or was not adjacent to profiles exhibiting CB1r immunoreactivity (37.4%; 175/468 profiles).

For peri-LC analysis, a total of 294 profiles were analyzed obtained from at least five grids per LC section. At least three LC sections were collected from each Sprague–Dawley rat ($n=3$). Of the 294 axon terminals analyzed that contained CRF, 35.37% (104/294 profiles) also contained CB1r, and of the 104 CRF + CB1r co-labeled axon terminals, and 10.2% (30/104 profiles) contacted dendrites that expressed CB1r postsynaptically. In addition, 6.46% (19/294 profiles) of CRF axon terminals that did not express CB1r synapsed onto dendrites that contained CB1r. The remainder of CRF terminals did not exhibit CB1r or were not adjacent to profiles exhibiting CB1r immunoreactivity (47.96%; 141/294 profiles). This provides compelling evidence for presynaptic regulation of CRF afferents by the eCB system in both the core and peri-LC areas.

CRF and CB1r co-localize at inhibitory and excitatory synapses in LC

The type of synapses formed by CRF-labeled axon terminals that either contain CB1r or apposed to CB1r-containing dendrites were subsequently analyzed. In the LC core, of the dually labeled CRF- and CB1r axon terminals that formed synapses with unlabeled dendrites (Fig. 4a–c), 72.0% (131/182 profiles) exhibited symmetric synapses (Fig. 4b), 17.0% (31/182 profiles) formed asymmetric synapses (Fig. 4c), and 11.0% (20/182 profiles) formed undefined synapses (Fig. 4a). For CRF-labeled axon terminals apposed to CB1r-labeled dendrites, 52.9% (45/85 profiles) formed symmetric synapses, 36.5% (31/85 profiles) formed asymmetric synapses, and 10.6% (9/85 profiles) formed undefined synapses. For dually labeled CRF- and CB1r axon terminals apposed to CB1r-labeled dendrites, 50.0% (13/26 profiles) formed symmetric synapses, 38.5% (10/26 profiles) formed asymmetric synapses, and 11.5% (3/26 profiles) formed undefined synapses.

In the peri-LC, of the dually labeled CRF- and CB1r axon terminals that formed synapses with unlabeled dendrites (Fig. 4d), 21.15% (22/104 profiles) formed symmetric synapses, 53.84% (56/104 profiles) formed asymmetric synapses (Fig. 4d), and 28.85% (30/104 profiles) formed undefined synapses. For CRF-labeled axon terminals apposed to CB1r-labeled dendrites, 21.05% (4/19 profiles) formed symmetric synapses, 57.89% (11/19 profiles) formed asymmetric synapses, and 21.05% (4/19 profiles) formed undefined synapses. For dual CRF- and CB1r-labeled terminals apposed to CB1r-labeled dendrites, 30.0% (9/30 profiles) formed symmetric synapses, 56.67% (17/30 profiles) formed asymmetric synapses, and 13.33% (4/30 profiles) formed undefined synapses. As compared to the core of the LC, where CB1r and CRF interactions exhibited primarily inhibitory-type synapses, the peri-LC showed a different synaptic organization with dually labeled terminals exhibiting primarily excitatory synapses.

The different morphological characteristics of dually labeled CRF and CB1r synaptic specializations in the core vs. peri-LC suggested that CB1r modulation of either inhibitory or excitatory CRF afferents. To further explicate the neurochemical signature of dually labeled CRF and CB1r synapses, triple labeling immunofluorescence was performed. In addition to staining for CRF and CB1r, GAD, the enzyme responsible for GABA synthesis in axon terminals (Fonnum et al. 1970), was used as a marker for GABAergic neurons (Fig. 5), and VGlut, a protein responsible for filling synaptic vesicles with glutamate (Fremeau et al. 2004), was used as a marker for glutamatergic neurons (Fig. 6). Figures 5 and 6 demonstrate immunocytochemical evidence that CB1r, CRF, and GAD or VGlut are co-localized, suggesting that CB1r and CRF are expressed at both excitatory and inhibitory synapses. In addition, Figs. 5 and 6 show co-localization between CB1r and CRF in axon terminals lacking GAD or VGlut, respectively, as well as evidence for CB1r and GAD or VGlut in axon terminals lacking CRF.

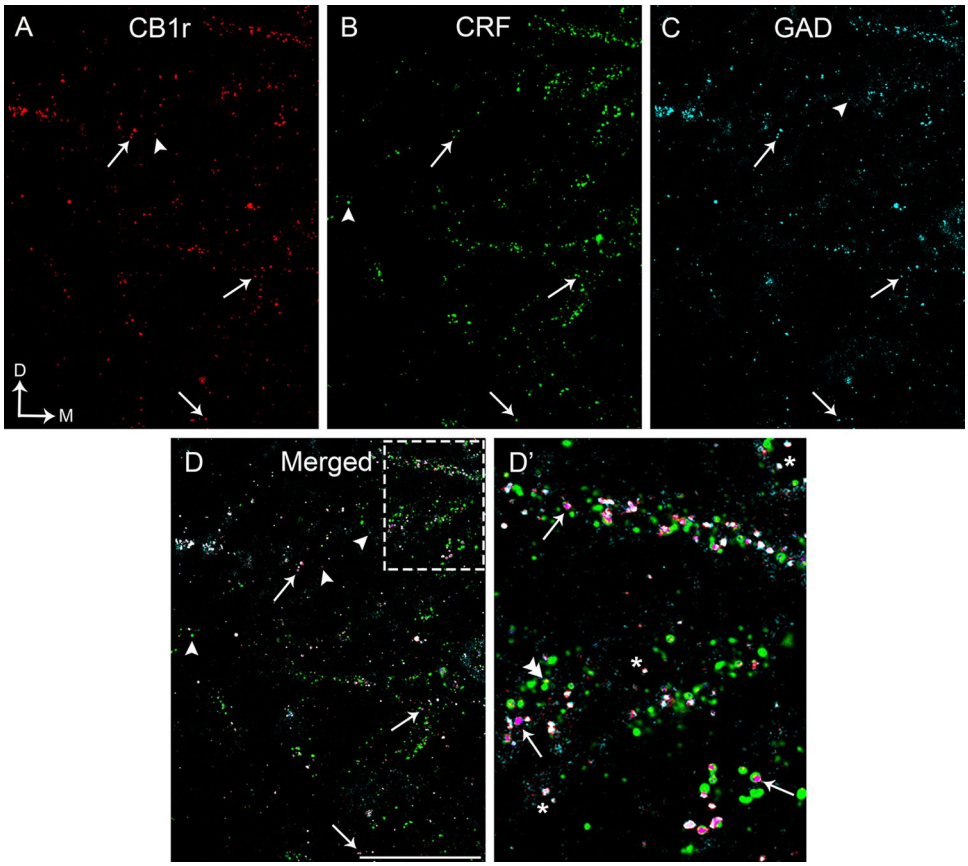

Fig. 5 CB1r and CRF co-localize with GAD in the LC. Confocal fluorescence micrographs showing CB1r (*red*), CRF (*green*), and GAD (*cyan*) co-localization in the LC. **a** CB1r was detected using a rhodamine isothiocyanate-conjugated secondary antibody. **b** CRF was detected using an Alexafluor 647-conjugated secondary antibody (pseudo-colored in *green*). **c** GAD was detected using a fluorescein isothiocyanate-conjugated secondary antibody (pseudocolored in *cyan*). **d** Triple co-localization (*pink*) can be seen in the *bottom row* and is depicted by *arrows*. The *inset* on the *bottom left panel* **d** is shown at a higher magnification on the *bottom right* (**d′**). In addition, co-localization of CB1r and CRF without GAD (*yellow, double arrowheads*) and CB1r and GAD without CRF (*white, asterisks*) is observed. *Single arrowheads* point to singly labeled CB1r, CRF, and GAD. *Scale bar* 30 µm

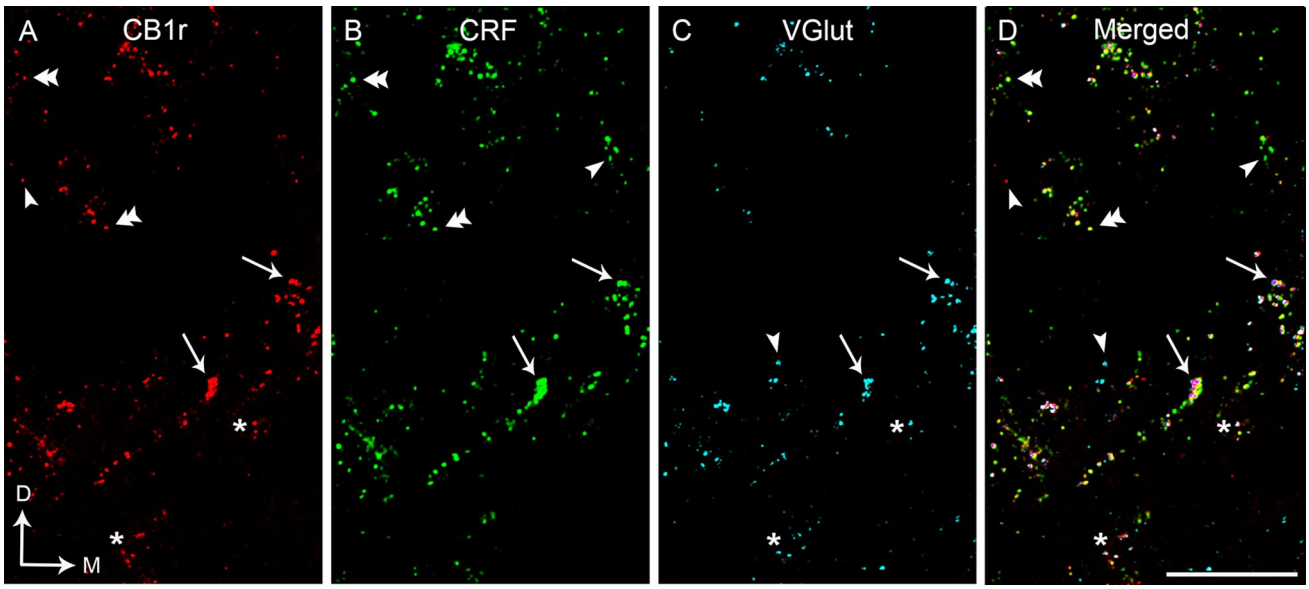

Fig. 6 CB1r and CRF co-localize with VGlut in the LC. Confocal fluorescence micrographs showing CB1r (*red*), CRF (*green*), and VGlut (*cyan*) co-localization in the LC. **a** CB1r was detected using a rhodamine isothiocyanate-conjugated secondary antibody. **b** CRF was detected using an Alexafluor 647-conjugated secondary antibody (pseudocolored in *green*). **c** VGlut was detected using a fluorescein isothiocyanate-conjugated secondary antibody (pseudocolored in *cyan*). **d** Triple co-localization (*pink*) can be seen in the *right panels* and is depicted by *arrows*. In addition, co-localization of CB1r and CRF without VGlut (*yellow, double arrowheads*) and CB1r and VGlut without CRF (*white, asterisks*) is observed. *Single arrowheads* point to singly labeled CB1r, CRF, and GAD. *Scale bar* 30 µm

CB1r and CRF co-localize in amygdalar projections to the LC

CRF afferents from both autonomic and limbic regions project to the LC, and the central nucleus of the amygdala (CeA) is one of the key limbic inputs involved in stress signaling (Aston-Jones et al. 1991; Van Bockstaele et al. 1996a, b, 1999). Previous electron microscopy tracing studies have shown that within the rostrolateral peri-LC, approximately 35% of axon terminals from the amygdala co-localize with CRF, and 22% of CRF-labeled profiles originate from the amygdala (Van Bockstaele et al. 1998). Anterograde transport of PHAL from the CeA (Fig. 7e) revealed that amygdalar projections to the LC that contain CRF also express CB1r (Fig. 7a–d), suggesting that CB1r are positioned to modulate amygdalar CRF release.

Discussion

While it is known that CRF and the eCB system independently regulate noradrenergic neurons in the LC, the present results demonstrate a direct interaction between the two by providing ultrastructural evidence for CB1r localization to CRF-containing axon terminals in the LC. To our knowledge, these findings provide the first anatomical evidence that the eCB system is positioned to directly modulate CRF stress-integrative circuitry within the LC-NE system. In addition, morphological analyses at the electron microscopic level revealed that dually labeled CB1r + CRF axon terminals exhibited Gray's Type I (asymmetric or excitatory type) and Gray's Type II (symmetric or inhibitory type) synapses. Interestingly, to our knowledge, this is the first subcellular evidence that CB1r and CRF are co-localized within the LC. Type I synapses were more frequently found in the peri-LC, a known source of CRF limbic afferents, while Type II synapses were more frequently localized in the core of the LC, a known source or autonomic and visceroreceptive afferents. The ultrastructural data were confirmed by a triple immunofluorescence labeling approach showing that dually labeled CRF and CB1r afferents contain markers for either excitatory or inhibitory-type amino acids. These results suggest that eCB modulation of CRF afferents will produce differential consequences on LC-neuronal activity depending on whether distinct CRF afferents that contain co-existing excitatory or inhibitory amino acid transmitters are engaged, and provide the first evidence that topographic distinctions occur between CB1r and CRF co-localization with inhibitory and excitatory amino acids in the core and peri-LC, respectively. Finally, co-localization of CB1r, CRF, and PHAL in the

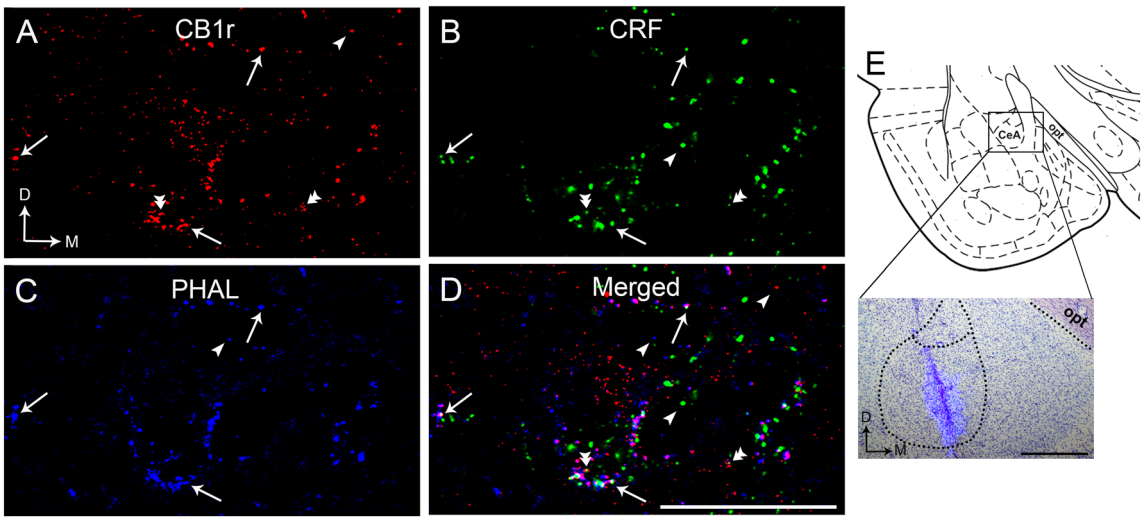

Fig. 7 CB1r and CRF co-localize in PHAL-labeled amygdalar afferents to the LC. The anterograde tracer PHAL was injected into the central nucleus of the amygdala (CeA) and immunofluorescence labeling was conducted for PHAL, CB1r and CRF in LC sections. **a–d** Confocal fluorescence micrographs demonstrate triple co-colocalization of CB1r, CRF, and PHAL in the peri-LC. CB1r was detected using a rhodamine isothiocyanate-conjugated secondary antibody **(a)** and CRF was detected using an Alexafluor 647-conjugated secondary antibody (pseudocolored in *green*) (**b**) and PHAL was detected using fluorescein isothiocyanate-conjugated secondary antibody (pseudocolored in *blue*) (**c**). **d** Triple co-localization (*white*) can be observed, and is depicted by *arrows*. *Double arrowheads* point to dual co-localization of CB1r and CRF (*yellow*). *Single arrowheads* point to singly labeled CB1r, CRF, and PHAL. *Scale bar* 25 µm. **e**. Schematic diagram adapted from the rat brain atlas of Paxinos and Watson (Paxinos and Watson 1997) depicting the location of the CeA. The *box* illustrates the region in which the lower image was taken. This image showing an overlay of fluorescein isothiocyanate-labeled PHAL injection site with the same section stained with Nissl shows that the injection was positioned in the CeA. *Opt* optic tract. *Scale bar* 0.5 mm

LC demonstrates that CB1r are localized in CRF-containing afferents that arise from the amygdala.

Methodological considerations

Dual labeling immunocytochemistry with peroxidase detection and immunogold–silver labeling combined with electron microscopy makes it possible to identify the subcellular localization of receptors within a defined neuronal population. However, some limitations need to be considered when interpreting results from pre-embedding immunoelectron microscopy experiments. Often, there is limited and/or differential penetration of the primary and secondary antibodies, especially in thicker tissue sections (Chan et al. 1990; Leranth and Pickel 1989). For example, antibodies directed against CRF or CB1r may not have penetrated the tissue section sufficiently, resulting in an underestimation of the number of CRF-containing afferents or CB1r in the LC. To minimize this caveat, only tissue sections where both markers could be detected near the tissue–Epon interface were analyzed (Leranth and Pickel 1989). In addition, while classifying synapses as symmetric or asymmetric at the electron microscopic level is suggestive of inhibitory or excitatory-type synapses (Gray 1959; Harris and Weinberg 2012), it is not definitive. Therefore, triple immunofluorescence using GAD as a marker for GABAergic synapses and VGlut as a marker for glutamatergic synapses was used to unequivocally establish the presence of inhibitory or excitatory amino acids in dually labeled CRF + CB1r afferents.

CRF regulation of LC neurons: implications for modulation by CB1r

The LC is a stress-integrative system that consists of a dense cluster of noradrenergic somata, defined as the core, with extensive dendritic processes extending from the core into surrounding portions of the neuropil, known as the peri-LC (Shipley et al. 1996). CRF fibers have been shown to prominently innervate peri-LC areas when compared to the core (Valentino et al. 2001; Van Bockstaele et al. 1996a, 1999). CRF-containing afferents originating from the central nucleus of the amygdala (CeA; Van Bockstaele et al. 1998), Barrington's nucleus (Bar; Valentino et al. 1996), the paraventricular nucleus of the hypothalamus (PVN; Reyes et al. 2005), and the nucleus paragigantocellularis (PGi; Van Bockstaele et al. 2001) form primarily asymmetric or excitatory-type synapses with LC dendrites. Additional CRF afferents arise from the BNST (Van Bockstaele et al. 1999), ventrolateral periaqueductal gray (PAG; Van Bockstaele et al. 2001), and the nucleus prepositus hypoglossi (PrH; Van Bockstaele et al. 2001) and form largely symmetric or inhibitory-type synapses (Fig. 8a). CRF afferents also exhibit topographic innervation of the LC core

A

Circuit	Co-localizing Amino Acid	Function	Effect of eCB System on LC Activity
CeA → LC	EAA	Emotionally-charged stimuli; fear	↓
PGi → LC	EAA	Autonomic and visceroceptive processing	↓
PrH → LC	GABA	Oculomotor functioning; REM sleep	↑
PVN → LC	EAA	HPA-axis activation; autonomic responses	↓

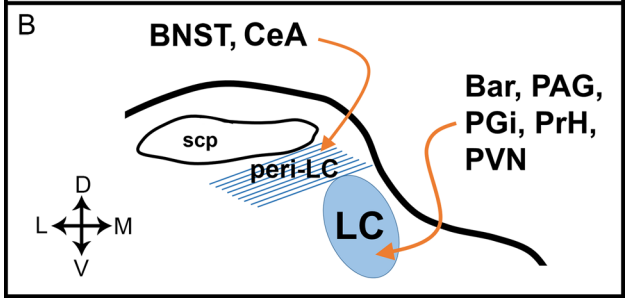

Fig. 8 Functional consequences of eCB modulation of CRF afferents. **a** Table showing known CRF projections to the LC, their putative co-localizing amino acid, and function. **b** Schematic depicting the topographic innervation of the LC by CRF afferents. *Bar, PAG, PGi, PrH*, and *PVN* are all known to project to the core of the LC, while the *BNST* and *CeA* project to the peri-LC

and peri-LC areas, with the CeA and BNST projecting to the peri-LC, while Bar, the PVN, PGi, PAG, and PrH, project to the core (Fig. 8b) (Van Bockstaele et al. 2001). CRF exerts a primarily postsynaptic regulation of LC neurons, where it acts upon CRF type 1 receptors that are prominently distributed within the LC (Curtis et al. 1999; Reyes et al. 2006a, 2008b).

During stress, CRF is released to shift the activity of LC neurons to a high tonic state that promotes scanning of the environment and behavioral flexibility (Curtis et al. 2001, 2002, 2012; Kreibich et al. 2008; Valentino et al. 2001; Valentino and Van Bockstaele 2005; Van Bockstaele et al. 2010; Xu et al. 2004). Previous neuroanatomical and electrophysiological studies demonstrated selective presynaptic inhibition of CRF afferent input by selective KOR agonists (Kreibich et al. 2008; Reyes et al. 2007). By allowing LC neurons to fire spontaneously, but attenuating information from excitatory afferents, presynaptic regulation of CRF by KOR may serve to protect the LC from over-activation (Kreibich et al. 2008). The present study reveals an additional component involved in the presynaptic regulation of CRF afferents in the LC, the CB1r. CB1r are known to be present in stress responsive circuits that are essential to the expression of stress-related behaviors (Hill et al. 2010; Shimizu et al. 2010). For example, the eCB system plays a critical role in glucocorticoid-mediated fast feedback inhibition of the HPA axis (Hill and McEwen 2009; Hill et al. 2010), and acute restraint stress has been shown to increase the synthesis

of endogenous eCB in limbic forebrain areas (Haller et al. 2002; Martin et al. 2002; Patel et al. 2005). CB1r agonist administration has been shown to alter LC-neuronal discharge and NE release in target regions during basal and stress conditions (Herkenham et al. 1990; Oropeza et al. 2005; Page et al. 2007, 2008; Reyes et al. 2012).

Ultrastructural analysis in the present study reveals that a majority of CRF and CB1r dual-labeled afferents in the peri-LC form Type I or asymmetric synapses, suggesting that the eCB system may modulate release of CRF from limbic afferents, such as the amygdala, which was confirmed by combining anterograde labeling from the CeA with immunofluorescence detection of CRF and CB1r. eCB signaling within the amygdala is necessary for habituation and adaptation of fear-related behaviors (Kamprath et al. 2006; Marsicano et al. 2002; Wyrofsky et al. 2015). It is tempting to speculate that eCB modulation of the amygdalar CRF afferents in the LC could also play a role in attenuating emotionally-charged stimuli. LC activation causes an increase in NE release in the mPFC, which plays a critical role in aversive memory extinction, and NE dysregulation can lead to the development of anxiety disorders (Wyrofsky et al. 2015; Mueller and Cahill 2010; Mueller et al. 2008). CRF release from the amygdala is known to increase LC activity. The co-localization of CB1r on amygdalar CRF afferents provides a potential mechanism for the eCB system to modulate the stress response and attenuate stress-induced dysregulation of frontal cortical activity, which may result in enhancing traumatic memory extinction and diminish anxiety-like behaviors.

A smaller percentage of CRF afferents co-expressing CB1r in the peri-LC formed Type II or symmetric synapses; therefore, the eCB system could also have an effect on CRF projections from the BNST. Unlike the peri-LC, a large majority of CB1r and CRF dual-labeled synapses in the core region were of the inhibitory type (Type II synapses). GABA + CRF afferents originate in regions responsible for providing sensory and autonomic stimuli to the LC (Aston-Jones et al. 1991; Samuels and Szabadi 2008; Van Bockstaele et al. 2001). LC-neuronal activity has a biphasic effect on arousal and attention: low tonic activity via involvement of GABA is associated with disengagement from the environment, while phasic activity is optimal for sustained focused attention (Aston-Jones 1985; Aston-Jones and Cohen 2005). High tonic activity correlates with a shift towards scanning the environment and heightened arousal (Aston-Jones and Cohen 2005; Berridge and Waterhouse 2003; Valentino and Van Bockstaele 2008b). While an initial shift to high tonic activity results in CRF-induced increases in behavioral engagement and scanning and is beneficial for adaptive responses to a stressor, chronic high tonic activity disrupts focused attention (Aston-Jones and Cohen 2005; Valentino and Van Bockstaele 2008b). In this regard, eCB modulation of CRF could act to return LC activity to optimal phasic levels.

In other brain regions, such as the hippocampus and cerebellum, it has been shown that CB1r can be located in the peri-synaptic region of both excitatory and GABAergic synapses (Kawamura et al. 2006; Nyiri et al. 2005). It is possible that further studies examining the regions adjacent to CRF afferents would reveal CB1r localization. Moreover, while CB1r is the predominant cannabinoid receptor in the brain (Scavone et al. 2010; Wyrofsky et al. 2015), eCBs can act at other receptors. Specifically, AEA has been shown to bind and activate transient receptor potential vanilloid type 1 receptors (TRPV1), resulting in long-term depression within the dentate gyrus in a CB1r-independent manner (Chavez et al. 2010; Ryskamp et al. 2014). TRPV1 expression has been reported in the LC (Caterina 2003; Toth et al. 2005). Future immunoelectron microscopy studies could examine the exact location of TRPV1 receptors, and if they are localized to excitatory CRF-containing terminals, they could represent another manner in which the eCB system could affect stress input from the PVN, Bar, and PGi.

In addition, our data demonstrate CB1r labeling in somatodendritic processes, consistent with our previous reports (Scavone et al. 2010). It is not clear whether these CB1r are functional within the LC or whether these are CB1r being transported to noradrenergic axon terminals in the frontal cortex. We have previously demonstrated that noradrenergic axon terminals in the prefrontal cortex exhibit CB1r (Oropeza et al. 2007) and LC neurons express CB1r mRNA (Tsou et al. 1998; Matsuda et al. 1993). Interestingly, there is evidence for functional postsynaptically distributed CB1 receptors in other brain regions. Cytoplasmic CB1r distribution has been observed within the rat caudate putamen nucleus (Rodriguez et al. 2001). In addition, in HEK-293 cells transfected with CB1r, ~85% of CB1r are localized in intracellular vesicles (Leterrier et al. 2004), and the changes in subcellular localization seem to be attributed to activation-dependent internalization via endosomes during steady-state conditions (Thibault et al. 2013). Ongoing slice physiology studies within the LC in our laboratory are exploring the functional significance of postsynaptically distributed CB1r (Wyrofsky et al. 2016). Therefore, future studies will provide critical information on the functional significance of pre- and postsynaptically distributed CB1r in the LC.

Functional implications

Targeting the eCB regulation of the LC-NE stress-integrative circuit could provide therapeutic relief for various stress-induced anxiety disorders (Wyrofsky et al. 2015). For example, the inability to extinguish aversive and fearful memories coupled with repeated re-consolidation of these

memories in limbic circuits underlies the pathophysiology of post-traumatic stress disorder (PTSD) and other anxiety disorders (Jovanovic and Ressler 2010; Lehner et al. 2009), and NE is involved in both processes. Consolidation of emotional memories involves LC-NE inputs to the amygdala (Ferry et al. 1999; McGaugh et al. 1996), while extinction of these memories involves LC-NE signaling in the mPFC (Mueller and Cahill 2010; Mueller et al. 2008). Several cannabinoid receptor ligands, including THC (an active component in cannabis) and nabilone (a synthetic cannabinoid ligand), have shown promise in clinical studies at reducing the symptoms and flashbacks associated with PTSD (Fraser 2009, US National Institutes of Health 2012), and many individuals suffering from PTSD self-medicate with cannabis (Passie et al. 2012).

Interestingly, cannabinoids are known to affect anxiety in a bidirectional and dose-dependent manner, with lower doses generally producing anxiolytic effects, while higher doses result in anxiogenesis (Rey et al. 2012; Trezza and Vanderschuren 2008; Viveros et al. 2005). A recent study using CB1r conditional knock out mice showed that CB1r activation on GABAergic neurons in the forebrain is necessary for the anxiogenic effects of cannabinoids, while CB1r activation on cortical glutamatergic neurons is necessary for the anxiolytic effects (Rey et al. 2012). It is tempting to speculate that a similar mechanism applies to eCB modulation of CRF afferents in the LC. We have previously shown that CB1r is positioned to modulate at symmetric and asymmetric synapses (Scavone et al. 2010). Moreover, using single-unit extracellular recordings has demonstrated that CB1r activation can modulate synaptic transmission within the LC via the glutamatergic and GABAergic systems (Muntoni et al. 2006; Mendiguren and Pineda 2004). While these data provide evidence of CB1r activation of LC through the excitatory and inhibitory neurotransmission, our present results are the first report illustrating the distribution and topography of CB1r modulation of glutamatergic and GABAergic CRF afferents not only at the immunofluorescence level but more importantly and interestingly at the ultrastructural level. In addition, this is the first report showing differential topography in synaptic signature of CB1r and CRF co-localization, where asymmetric synapses indicative of excitatory transmission predominate in the peri-LC and symmetric synapse predominates in LC core indicative of inhibitory transmission. CRF afferents co-localizing CB1r in the peri-LC and forming asymmetric synapses suggest co-localization with glutamate (Van Bockstaele et al. 1996a, 1999), and we have shown CB1r and CRF co-localization within afferents originating from the amygdala, a brain region responsible for providing fear-related stimuli and emotional input (Davis 1992; Kamprath et al. 2006; Walker et al. 2003). Blocking signaling from the amygdala via CB1r activation in the peri-LC could contribute to cannabinoid-induced anxiolytic effects. Because dysregulation of NE in the mPFC is known to contribute to the development of anxiety disorders (Anand and Charney 2000; Carvalho and Van Bockstaele 2012; Itoi and Sugimoto 2010; Nutt 2006; Southwick et al. 1999), targeting the eCB modulation of CRF afferents in the LC during stress may underlie the efficacy of nabilone in PTSD patients.

References

Abou-Samra AB, Catt KJ, Aguilera G (1986) Biphasic inhibition of adrenocorticotropin release by corticosterone in cultured anterior pituitary cells. Endocrinology 119:972–977

Adler J and Parmryd I (2010) Quantifying colocalization by correlation: the Pearson correlation coefficient is superior to the Mander's overlap coefficient. J Int Soc Adv Cytom 77A(8):733–742

Anand A, Charney DS (2000) Norepinephrine dysfunction in depression. J Clin Psychiatry 61:16–24

Aston-Jones G (1985) Behavioral functions of locus coeruleus derived from cellular attributes. Physiol Psychol 13:118–126

Aston-Jones G, Cohen JD (2005) An integrative theory of locus coeruleus-norepinephrine function: adaptive gain and optimal performance. Annu Rev Neurosci 28:403–450

Aston-Jones G, Shipley MT, Chouvet D, Ennis M, Van Bockstaele EJ, Pieribone V, Shiekhatter R, Akaoka H, Drolet G, Astier B (1991) Afferent regulation of locus coeruleus neurons: anatomy, physiology and pharmacology. Prog Brain Res 88:47–75

Bergamaschi MM, Queiroz RH, Chagas MH, de Oliveira DC, De Martinis BS, Kapczinski F, Quevedo J, Roesler R, Schroder N, Nardi AE, Martin-Santos R, Hallak JE, Zuardi AW, Crippa JA (2011) Cannabidiol reduces the anxiety induced by simulated public speaking in treatment-naive social phobia patients. Neuropsychopharmacology 36:1219–1226

Berridge CW, Waterhouse BD (2003) The locus coeruleus-noradrenergic system: modulation of behavioral state and state-dependenge cognitive processes. Brain Res Rev 43:33–84

Carvalho AF, Van Bockstaele EJ (2012) Cannabinoid modulation of noradrenergic circuits: Implications for psychiatric disorders. Prog Neuropsychopharmacol Biol Psychiatry 38:59–67

Carvalho AF, Mackie K, Van Bockstaele EJ (2010) Cannabinoid modulation of limbic forebrain noradrenergic circuitry. Eur J Pharmacol 31:286–301

Castillo PE, Younts TJ, Chavez AE, Hashimotodani Y (2012) Endocannabinoid signaling and synaptic function. Neuron 76:70–81

Caterina MJ (2003) Vanilloid receptors take a TRP beyond the sensory afferent. Pain 105:5–9

Chan J, Aoki C, Pickel VM (1990) Optimization of differential immunogold-silver and peroxidase labeling with maintenance of ultrastructure in brain sections before plastic embedding. J Neurosci Methods 33:113–127

Chavez AE, Chiu CQ, Castillo PE (2010) TRPV1 activation by endogenous anandamide triggers postsynaptic long-term depresison in dentate gyrus. Nat Neurosci 13:1511–1518

Cota D (2008) The role of the endocannabinoid system in the regulation of the hypothalamic-pituitary-adrenal axis activity. J Neuroendocrinol 20:35–38

Curtis A, Lechner SM, Pavcovich LA, Valentino RJ (1996) Activation of the locus coeruleus noradrenergic system by intracoerulear microinfusion of corticotropin-releasing factor: effects on discharge rate, cortical norepinephrine levels and cortical electroencephalographic activity. J Pharmacol Exp Ther 281:163–172

Curtis A, Pavcovich LA, Valentino RJ (1999) Long-term regulation of locus ceruleus sensitivity to corticotropin-releasing factor by swim stress. J Pharmacol Exp Therap 289:1211–1219

Curtis A, Bello NT, Valentino RJ (2001) Evidence for functional release of endogenous opioids in the locus ceruleus during stress termination. J Neurosci 21:1–5

Curtis AL, Bello NT, Connolly KR, Valentino RJ (2002) Corticotropin-releasing factor neurones of the central nucleus of the amygdala mediate locus coeruleus activation by cardiovascular stress. J Neuroendocrinol 14:667–682

Curtis A, Leiser SC, Snyder K, Valentino RJ (2012) Predator stress engages corticotropin-releasing factor and opioid systems to alter the operating mode of locus coeruleus norepinephrine neurons. Neuropharmacology 62:1737–1745

Davis M (1992) The role of the amygdala in fear and anxiety. Annu Rev Neurosci 15:353–375

Derbenev AV, Stuart TC, Smith BN (2004) Cannabinoids suppress synaptic input to neurones of the rat dorsal motor nucleus of the vagus nerve. J Physiol 559:923–938

Di Marzo V, Bifulco M, De Petrocellis L (2004) The endocannabinoid system and its therapeutic exploitation. Nat Rev Drug Discov 3:771–784

Edelmann L, Hanson PI, Chapman ER, Jahn R (1995) Synaptobrevin binding to synaptophysin: a potential mechanism for controlling the exocytotic fusion machine. EMBO J 14:224–231

Ferry B, Roozendaal B, McGaugh JL (1999) Role of norepinephrine in mediating stress hormone regulation of long-term memory storage: a critical involvement of the amygdala. Biol Psychiatry 46:1140–1152

Fonnum F, Storm-Mathisen J, Walberg F (1970) Glutamate decarboxylase in inhibitory neurons: a study of the enzyme in purkinje cell axons and boutons in the cat. Brain Res 20:259–275

Fraser GA (2009) The use of a synthetic cannabinoid in the management of treatment-resistant nightmares in posttraumatic stress disorder (PTSD). CNS Neurosci Therap 15:84–88

Fremeau j RT, Kam K, Qureshi T, Johnson J, Copenhagen DR, Storm-Mathisen J, Chaudhry FA, Nicoll RA, Edwards RH (2004) Vesicular glutamate transporters 1 and 2 target to functionally distinct synaptic release sites. Science 304:1815–1819

Freund TF, Katona I, Piomelli D (2003) Role of endogenous cannabinoids in synaptic signaling. Physiol Rev 83:1017–1066

Gobbi G, Bambico FR, Mangieri R, Bortolato M, Campolongo P, Solinas M, Cassano T, Morgese MG, Debonnel G, Duranti A, Tontini A, Tarzia G, Mor M, Trezza V, Goldberg SR, Cuomo V, Piomelli D (2005) Antidepressant-like activity and modulation of brain monoaminergic transmission by blockade of anandamide hydrolysis. Proc Natl Acad Sci USA 102:18620–18625

Gray EG (1959) Axosomatic and axo-dendritic synapses of the cerebral cortex: an electron microscopic study. J Anat 93:420–433

Haller J, Bakos N, Szirmay M, Ledent C, Freund TF (2002) The effects of genetic and pharmacological blockade of the CB1 cannabinoid receptor on anxiety. Eur J Neurosci 16:1395–1398

Harris KM and Weinberg RJ (2012) Ultrastructure of synapses in the mammalian brain. Cold Spring Harbor Perspect Biol 4

Heilig M (2004) The NPY system in stress, anxiety and depression. Neuropeptides 38:213–224

Herkenham M, Lynn AB, Little MD, Johnson MR, Melvin LS, de Costa BR, Rice KC (1990) Cannabinoid receptorl localization in brain. Proc Natl Acad Sci USA 87:1932–1936

Herkenham M, Lynn AB, Johnson MR, Melvin LS, de Costa BR, Rice KC (1991) Characterization and localization of cannabinoid receptors in rat brain: a quantitative in vitro autoradiographic study. J Neurosci 11:563–583

Herman JP, Cullinan WE (1997) Neurocircuitry of stress: central control of the hypothalmo–pituitary–adrenocortical axis. Trends Neurosci 20:78–84

Hill MN, McEwen BS (2009) Endocannabinoids: the silent partner of glucocorticoids in the synapse. Proc Natl Acad Sci 106:4579–4580

Hill MN, Patel S, Campolongo P, Tasker JG, Wotjak CT, Bains JS (2010) Functional interactions between stress and the endocannabinoid system: from synaptic signaling to behavioral output. J Neurosci 30:14980–14986

Itoi K, Sugimoto N (2010) The brain noradrenergic systems in stress, anxiety, and depression. J Neuroendocrinol 22:355–361

Javadi P, Bouskila J, Bouchard J-P, Ptito M (2015) The endocannabinoid system within the dorsal lateral geniculate nucleus of the vervet monkey. Neuroscience 288:135–144

Jovanovic T, Ressler KJ (2010) How the neurocircuitry and genetics of fear inhibition may inform our understanding of PTSD. Am J Psychiatry 167:648–662

Kamprath K, Marsicano G, Tang J, Monory K, Bisogno T, Di Marzo V, Lutz B, Wotjak CT (2006) Cannabinoid CB1 receptor mediates fear extinction via habituation-like processes. J Neurosci 26:6677–6686

Kawamura Y, Fukaya M, Maejima T, Yoshida T, Miura E, Watanabe M, Ohno-Shosaku T, Kano M (2006) The CB1 cannabinoid receptor is the major cannabinoid receptor at excitatory presynaptic sites in the hippocampus and cerebellum. J Neurosci 26:2991–3001

Keller-Wood ME and Dallman MF (1984) Corticosteroid inhibition of ACTH secretion. Endocr Rev:51–24

Kreibich A, Reyes BA, Curtis A, Ecke L, Chavkin C, Van Bockstaele EJ, Valentino RJ (2008) Presynaptic inhibition of diverse afferents to the locus ceruleus by K-opiate receptors: a novel mechanism for regulating the central norepinephrine system. J Neurosci 28:6516–6525

Lehner M, Wilslowska-Stanek A, Plaznik A (2009) Extinction of emotional response as a novel approach of pharmacotherapy of anxiety disorders. Psychiatr Pol 43:639–653

Leranth C, Pickel VM (1989) Electron microscopic preembedding double-labeling methods. In: Heimer L, Zaborszky L (eds) Neuroanatomical tracing methods 2, 1st edn. Plenum Press, New York, pp 129–172

Leterrier C, Bonnard D, Carrel D, Rossier J, Lenkei Z (2004) Constitutive endocytic cycle of the CB1 cannabinoid receptor. J Biol Chem 279:36013–36021

Mailleux P, Vanderhaeghen J-J (1992) Distribution of neuronal cannabinoid receptor in the adult rat brain: a comparative receptor binding autoradiography and in situ hybridization histochemistry. Neuroscience 48:655–668

Marsicano G, Wotjak CT, Azad SC, Bisogno T, Rammes G, Cascio MG, Hermann H, Tang J, Hofmann C, Zieglgansberger W, Di Marzo V, Lutz B (2002) The endogenous cannabinoid system controls extinction of aversive memories. Nature 481:530–534

Martin M, Ledent C, Parmentier M, Maldonado R, Valverde O (2002) Involvement of CB1 cannabinoid receptors in emotional behavior. Psychopharmacology (Berl) 159:379–387

Matsuda LA, Bonner TI, Lolait SJ (1993) Localization of cannabinoid receptor mRNA in rat brain. J Comp Neurol 327:535–550

McGaugh JL, Cahill L, Roozendaal B (1996) Involvement of the amygdala in memory storage: interaction with other brain systems. Proc Natl Acad Sci USA 93:13508–13514

Mendiguren A, Pineda J (2004) Cannabinoids enhance *N*-methyl-D-aspartate-induced excitation of locus coeruleus neurons by CB(1) receptors in rat brain slices. Neurosci Lett 363:1–5

Mendiguren A, Pineda J (2006) Systemic effect of cannabinoids on the spontaneous firing rate of locus coeruleus neurons in rats. Eur J Pharmacol 534:83–88

Mendiguren A, Pineda J (2007) CB1 cannabinoid receptors inhibit the glutamatergic component of KCl-evoked excitation of

locus coeruleus neurons in rat brain slices. Neuropharmacology 52:617–625
Moranta D, Esteban S, Garcia-Sevilla JA (2009) Chronic treatment and withdrawal of the cannabinoid agonist WIN 55,212-2 modulate the sensitivity of presynaptic receptors involved in the regulation of monoamine syntheses in rat brain. Naunyn Schmiedebergs Arch Pharmacol 379:61–72
Mueller D, Cahill SP (2010) Noradrenergic modulation of extinction learning and exposure therapy. Behav Brain Res 208:1–11
Mueller D, Porter JT, Quirk GJ (2008) Noradrenergic signaling in infralimbic cortex increases cell excitability and strengthens memory for fear extinction. J Neurosci 28:369–375
Muntoni AL, Pillolla G, Melis M, Perra S, Gessa GL, Pistis M (2006) Cannabinoids modulate spontaneous neuronal activity and evoked inhibition of locus coeruleus noradrenergic neurons. Eur J Pharmacol 23:2385–2394
Nutt DJ (2006) The role of dopamine and norepinephrine in depression and antidepressant treatment. J Clin Psychiatry 67:3–8
Nyiri G, Cserep C, Szabadits E, Mackie K, Freund TF (2005) CB1 cannabinoid receptors are enriched in the perisynaptic annulus and on preterminal segments of hippotampal GABAergic axons. Neuroscience 136:811–822
Oropeza VC, Page ME, Van Bockstaele EJ (2005) Systemic administration of WIN 55,212-2 increases norepinephrine release in the rat frontal cortex. Brain Res 1046:45–54
Oropeza VC, Mackie K, Van Bockstaele EJ (2007) Cannabinoid receptors are localized to noradrenergic azon terminals in the rat frontal cortex. Brain Res 1127:36–44
Page ME, Oropeza VC, Sparks SE, Qian Y, Menko AS, Van Bockstaele EJ (2007) Repeated cannabinoid administration increases indices of noradrenergic activity in rats. Pharmacol Biochem Behav 86:162–168
Page ME, Oropeza VC, Van Bockstaele EJ (2008) Local administration of a cannabinoid agonist alters norepinephrine efflux in the rat frontal cortex. Neurosci Lett 431:1–5
Papay R, Gaivin R, Jha A, McCune DF, McGrath JC, Rodrigo MC, Simpson PC, Doze VA, Perez DM (2006) Localization of the mouse $a1_A$-adrenergic receptor (AR) in the brain: $a1_A$AR is expressed in neurons, GABAergic interneurons, and NG2 oligodendrocyte progenitors. J Comp Neurol 497:209–222
Passie T, Emrich HM, Karst M, Brandt SD, Halpern JH (2012) Mitigation of post-traumatic stress symptoms by Cannabis resin: a review of the clinical and neurobiological evidence. Drug Test Anal 4:649–659
Patel KD, Hillard CJ (2003) Cannabinoid-induced fos expression within A10 dopaminergic neurons. Brain Res 963:15–25
Patel S, Roelke CT, Rademacher DJ, Hillard CJ (2005) Inhibition of restraint stress-induced neural and behavioral activation by endogenous cannabinoid signaling. Eur J Neurosci 21:1057–1069
Paxinos G and Watson C (1997) The rat brain in stereotaxic coordinates, 3rd edn. Academic, San Diego
Peters A, Palay SL (1996) The morphology of synapses. J Neurocytol 25:687–700
Plotsky PM, Owens MJ, Nemeroff CB (1998) Psychoneuroendocrinology of depression: hypothalamic–pituitary–adrenal axis. Psychiatr Clin N Am 21:293–307
Rey AA, Purrio M, Viveros MP, Lutz B (2012) Biphasic effects of cannabinoids in anxiety responses: CB1 and GABAB receptors in the balance of GABAergic and glutamatergic neurotransmission. Neuropsychopharmacology 37:2624–2634
Reyes BA, Valentino RJ, Xu G, Van Bockstaele EJ (2005) Hypothalamic projections to locus coeruleus neurons in rat brain. Eur J Neurosci 22:93–106
Reyes BA, Fox K, Valentino RJ, Van Bockstaele EJ (2006a) Agonist-induced internalization of corticotropin-releasing factor receptors in noradrenergic neurons of the rat locus coeruleus. Eur J Neurosci 23:2991–2998
Reyes BA, Glaser JD, Magtoto R, Van Bockstaele EJ (2006b) Pro-opiomelanocortin colocalizes with corticotropin- releasing factor in axon terminals of the noradrenergic nucleus locus coeruleus. Eur J Neurosci 23:2067–2077
Reyes BA, Johnson AD, Glaser JD, Commons KG, Van Bockstaele EJ (2007) Dynorphin-containing axons directly innervate noradrenergic neurons in the rat nucleus locus coeruleus. Neuroscience 145:1077–1086
Reyes BA, Drolet G, Van Bockstaele EJ (2008a) Dynorphin and stress-related peptides in rat locus coeruleus: contribution of amygdalar efferents. J Comp Neurol 508:663–675
Reyes BA, Valentino RJ, Van Bockstaele EJ (2008b) Stress-induced intracellular trafficking of corticotropin-releasing factor receptors in rat locus coeruleus neurons. Endocrinology 149:122–130
Reyes BA, Carvalho AF, Vakharia K, Van Bockstaele EJ (2011) Amygdalar peptidergic circuits regulating noradrenergic locus coeruleus neurons: linking limbic and arousal centers. Exp Neurol 230:96–105
Reyes BA, Szot P, Sikkema C, Cathel AM, Kirby LG, Van Bockstaele EJ (2012) Stress-induced sensitization of cortical adrenergic receptors following a history of cannabinoid exposure. Exp Neurol 236:327–335
Rodriguez JJ, Mackie K, Pickel VM (2001) Ultrastructural localization of the CB1 cannabinoid receptor in u-opioid receptor patches of the rat caudate putamen nucleus. J Neurosci 21(3):823–833
Rubio-Aliaga I, Boll M, Weisenhorn DMV, Foltz M, Kottra G, Daniel H (2004) The proton/amino acid cotransporter PAT2 is expressed in neurons with a different subcellular localization that its paralog PAT1. J Biol Chem 279(4):2754–2760
Rudoy CA, Reyes BA, Van Bockstaele EJ (2009) Evidence for beta1-adrenergic receptor involvement in amygdalar corticotropin-releasing factor gene expression: implications for cocaine withdrawal. Neuropsychopharmacology 35(5):1135–1148
Ryskamp DA, Redmon S, Jo AO, Krizaj D (2014) TRPV1 and endocannabinoids: emerging molecular signals that modulate mammalian vision. Cells 3:914–938
Samuels ER, Szabadi E (2008) Functional neuroanatomy of the noradrenergic locus coeruleus: its roles in the regulation of arousal and autonomic function part I: principles of functional organisation. Curr Neuropharmacol 6:235–253
Scavone JL, Mackie K, Van Bockstaele EJ (2010) Characterization of cannabinoid-1 receptors in the locus coeruleus: relationship with mu-opioid receptors. Brain Res 1312:18–31
Shimizu T, Lu L, Yokotani K (2010) Possible inhibitory roles of endogenous 2-arachidonoylglycerol during corticotropin-releasing factor-induced activation of central sympatho-adrenomedullary outflow in anesthetized rats. Eur J Pharmacol 641:54–60
Shipley MT, Fu L, Ennis M, Liu WL, Aston-Jones G (1996) Dendrites of locus coeruleus neurons extend preferentially into two pericoerulear zones. J Comp Neurol 365:56–68
Southwick SM, Bremner JD, Rasmusson A, Morgan CA III, Arnsten A, Charney DS (1999) Role of norepinephrine in the pathophysiology and treatment of posttraumatic stress disorder. Biol Psychiatry 46:1192–1204
Thibault K, Carrel D, Bonnard D, Gallatz K, Simon A, Biard M, Pezet S, Palkovits M, Lenkei Z (2013) Activation-dependent subcellular distribution patterns of CB1 cannabinoid receptors in the rat forbrain. Cereb Cortex 23(11):2581–2591
Tjoumakaris SI, Rudoy CA, Peoples J, Valentino RJ, Van Bockstaele EJ (2003) Cellular interactions between axon terminals containing endogenous opioid peptides or corticotropin-releasing factor in the rat locus coeruleus and surrounding dorsal pontine tegmentum. J Comp Neurol 466:445–456

Torner L, Toschi N, Pohlinger A, Landgraf R, Neumann ID (2001) Anxiolytic and anti-stress effects of brain prolactin: improved efficacy of antisense targeting of the prolactin receptor by molecular modeling. J Neurosci 21:3207–3214

Toth A, Boczan J, Kedei N, Lizanecz E, Bagi Z, Papp Z, Edes I, Csiba L, Blumberg PM (2005) Expression and distribution of vanilloid receptor 1 (TRPV1) in the adult rat brain. Mol Brain Res 135:162–168

Tournier M, Sorbara F, Gindre C, Swendsen JD, Verdoux H (2003) Cannabis use and anxiety in daily life: a naturalistic investigation in a non-clinical population. Psychiatry Res 118:1–8

Trezza V, Vanderschuren LJMJ (2008) Bidirectional cannabinoid modulation of social behavior in adolescent rats. Psychopharmacology (Berl) 197:217–227

Tsou K, Brown S, Sanudo-Pena MC, Mackie K, Walker JM (1998) Immunohistochemical distribution of cannabinoid CB1 receptors in the rat central nervous system. Neuroscience 83(2):393–411

Ulrich-Lai YM, Herman JP (2009) Neural regulation of endocrine and autonomic stress responses. Nat Rev Neurosci 10:397–409

US National Institutes of Health (2012) Add on Study on d9-THC Treatment for Posttraumatic Stress Disorders (PTSD) (THC_PTSD). Hadassah Medical Organization, Bethesda, MD. National Library of Medicine (US). http://clinicaltrials.gov/show/NCT00965809. NLM Identifier: NCT00965809. Accessed 3 Mar 2016

Vale W, Spiess J, Rivier CL, Rivier J (1981) Characterization of a 41-residue ovine hypothalamic peptide that stimulates secretion of cortico-tropin and beta-endorphin. Science 213:1394–1397

Valentino RJ (1988) CRH effects on central noradrenergic neurons: relationship to stress. Adv Exp Med Biol 245:47–64

Valentino RJ, Van Bockstaele EJ (2001) Opposing regulation of the locus coeruleus by corticotropin-releasing factor and opioids. Psychopharmacology (Berl) 158:331–342

Valentino RJ, Van Bockstaele EJ (2005) Functional interactions between stress neuromediators and the locus coeruleus-norepinephrine system. Tech Behav Neural Sci 15:465–486

Valentino RJ, Van Bockstaele E (2008a) Convergent regulation of locus coeruleus activity as an adaptive response to stress. Eur J Pharmacol 583:194–203

Valentino RJ, Van Bockstaele EJ (2008b) Convergent regulation of locus coeruleus activity as an adaptive response to stress. Eur J Pharmacol 583:194–203

Valentino RJ, Page ME, Van Bockstaele EJ, Aston-Jones G (1992) Corticotropin-releasing factor innervation of the locus coeruleus region: distribution of fibers and sources of input. Neuroscience 48:689–705

Valentino RJ, Sheng C, Yan Z, Aston-Jones G (1996) Evidence for divergent projections to the brain noradrenergic system and the spinal parasympathetic system from Barrington's nucleus. Brain Res 732:1–15

Valentino RJ, Rudoy CA, Saunders A, Liu XB, Van Bockstaele EJ (2001) Corticotropin-releasing factor is preferentially colocalized with excitatory rather than inhibitory amino acids in axon terminals in the peri-locus coeruleus region. Neuroscience 106:375–384

Valentino RJ, Foote SL, Page ME (2006) The locus coeruleus as a site for integrating corticotropin-releasing factor and noradrenergic mediation of stress responses. Ann N Y Acad Sci 697:173–188

Van Bockstaele EJ, Pickel VM (1993) Ultrastructure of serotonin-immunoreactive terminals in the core and shell of the rat nucleus accumbens: cellular substrates for interactions with catecholamine afferents. J Comp Neurol 334(4):603–617

Van Bockstaele EJ, Chan J, Pickel VM (1996a) Input from central nucleus of the amygdala efferents to pericoerulear dendrites, some of which contain tyrosine hydroxylase immunoreactivity. J Neurosci 45:289–302

Van Bockstaele EJ, Colago EE, Valentino RJ (1996b) Corticotropin-releasing factor-containing axon terminals synapse onto catecholamine dendrites and may presynaptically modulate other afferents in the rostral pole of the nucleus locus coeruleus in the rat brain. J Comp Neurol 364:523–534

Van Bockstaele EJ, Colago EEO, Valentino RJ (1998) Amygdaloid corticotropin-releasing factor targets locus coeruleus dendrites: substrate for the coordination of emotional and cognitive limbs of the stress response. J Neuroendocrinol 10:743–757

Van Bockstaele EJ, Peoples J, Valentino RJ (1999) Anatomic basis for differential regulation of the rostrolateral peri-locus coeruleus region by limbic afferents. Biol Psychiatry 46:1352–1363

Van Bockstaele EJ, Saunders A, Commons KG, Liu XB, Peoples J (2000) Evidence for coexistence of enkephalin and glutamate in axon terminals and cellular sites for functional interactions of their receptors in the rat locus coeruleus. J Comp Neurol 417:103–114

Van Bockstaele EJ, Bajic D, Proudfit H, Valentino RJ (2001) Topographic architecture of stress-related pathways targeting the noradrenergic locus coeruleus. Physiol Behav 73:273–283

Van Sickle MD, Duncan M, Kingsley PJ, Mouihate A, Urbani P, Mackie K, Stella N, Makriyannis A, Piomelli D, Davison JS, Marnett LJ, Di Marzo V, Pittman QJ, Patel KD, Sharkey KA (2005) Identification and functional characterization of brainstem cannabinoid CB2 receptors. Science 310:329–332

Van Bockstaele EJ, Reyes BA, Valentino RJ (2010) The locus coeruleus: a key nucleus where stress and opioids intersect to mediate vulnerability to opiate abuse. Brain Res 1314:162–174

Viveros MP, Marco EM, File SE (2005) Endocannabinoid system and stress and anxiety responses. Pharmacol Biochem Behav 81:331–342

Viveros MP, Marco EM, Llorente R, Lopez-Gallardo M (2007) Endocannabinoid system and synaptic plasticity: implications for emotional responses. Neural Plast 2007:52908

Walker DL, Toufexis DJ, Davis M (2003) Role of bed nucleus of the stria terminalis versus the amygdala in fear, stress, and anxiety. Eur J Pharmacol 463:199–216

Wingenfeld K, Wolf OT (2011) HPA axis alterations in mental disorders: impact on memory and its relevance for therapeutic interventions. CNS Neurosci Therap 17:714–722

Wyrofsky RR, McGonigle P, Van Bockstaele EJ (2015) Drug discovery strategies that focus on the endocannabinoid signaling system in psychiatric disease. Expert Opin Drug Discov 10:17–36

Wyrofsky RR, Reyes BA, Kirby LG and Van Bockstaele EJ (2016) Modulation of corticotropin-releasing factor-induced activation of noradrenergic neurons by a cannabinoid type 1 receptor agonist. Soc Neurosci

Xu G-P, Van Bockstaele EJ, Reyes BA, Bethea TT, Valentino RJ (2004) Chronic morphine sensitizes the brain norepinephrine system to corticotropin-releasing factor and stress. J Neurosci 24:8193–8197

Yamanaka H, Kobayashi K, Okubo M, Fukuoka T, Noguchi K (2011) Increase of close homolog of cell adhesion molecule L1 in primary afferent by nerve injury and the contribution to neuropathic pain. J Comp Neurol 519(8):1597–1615

Zuardi AW (2006) History of cannabis as a medicine: a review. Rev Bras Psiquiatr 28:153–157